

Supplementary figures to: Gaviria-Lugo et al. (Submitted) Climatic controls on leaf wax hydrogen isotope ratios in terrestrial and marine sediments along a hyperarid to humid gradient.

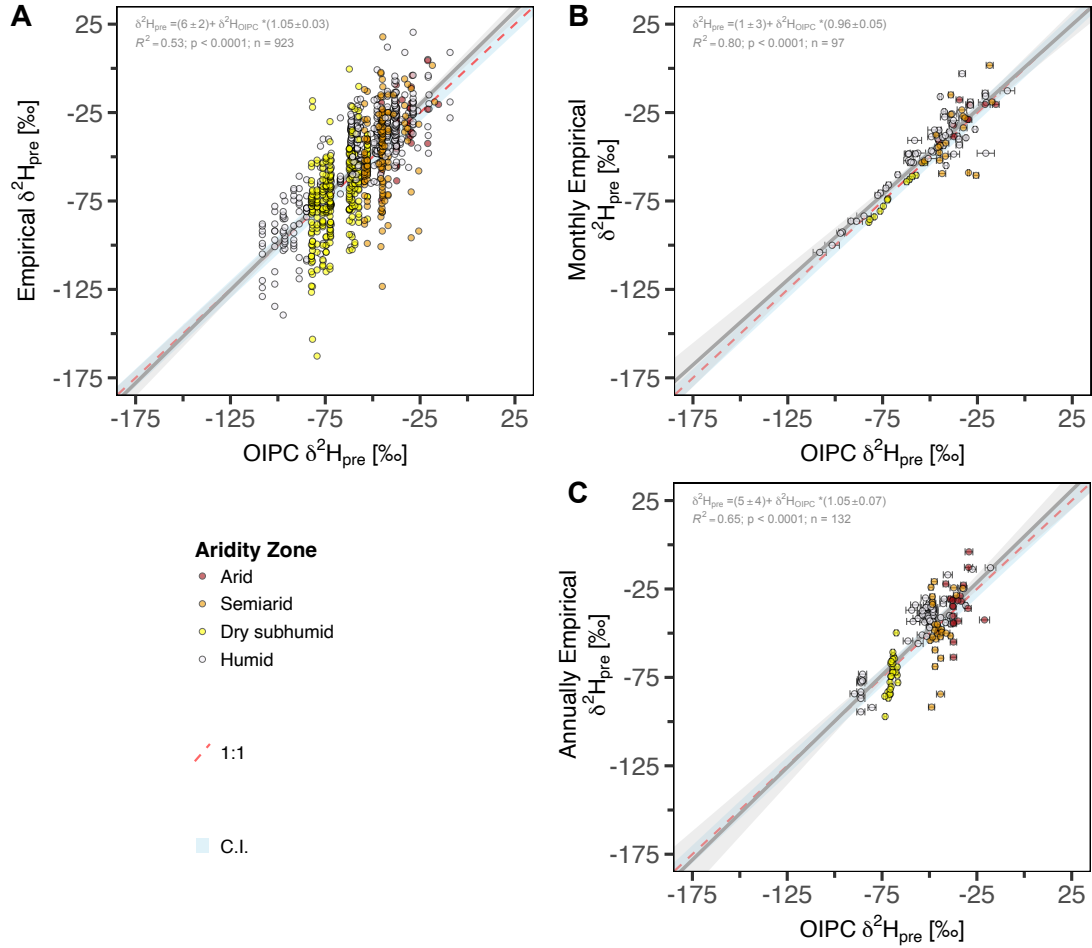


Figure S1. Measured $\delta^2\text{H}_{\text{pre}}$ vs predicted $\delta^2\text{H}_{\text{pre}}$ from the OIPC (Bowen and Revenaugh, 2003). The measured $\delta^2\text{H}_{\text{pre}}$ was acquired at 9 long term stations located along the different aridity zones of Chile (IAEA/WMO, 2023). **A.** Considering all month $\delta^2\text{H}_{\text{pre}}$ values registered for each station. **B.** Considering the long-term $\delta^2\text{H}_{\text{pre}}$ average values for each month at every station. **C.** Considering the long-term $\delta^2\text{H}_{\text{pre}}$ average values for each month at every station. **D.** Considering the long-term $\delta^2\text{H}_{\text{pre}}$ average values for each year at every station.

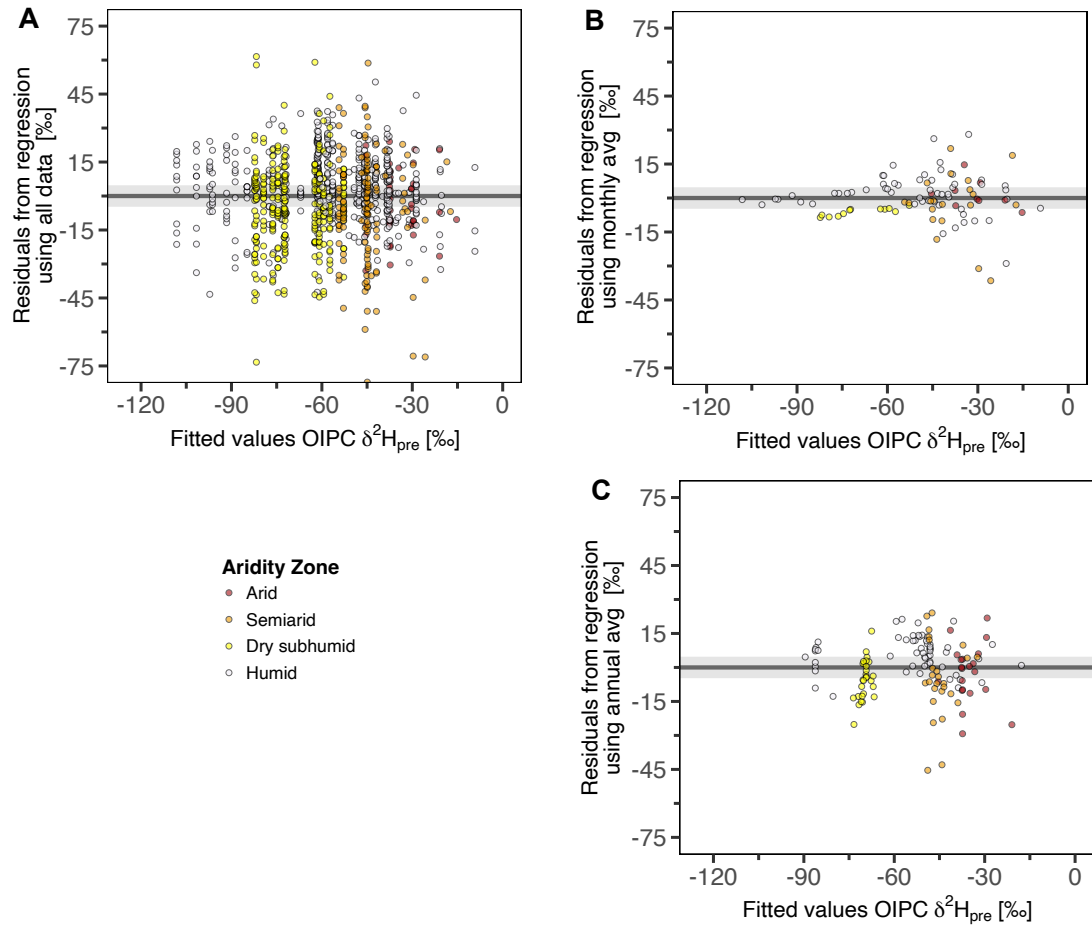


Figure S2. Residual plots for the different linear regressions fitted between the measured $\delta^2\text{H}_{\text{pre}}$ vs predicted $\delta^2\text{H}_{\text{pre}}$ from the OIPC (Bowen and Revenaugh, 2003) (Fig. S1). The measured $\delta^2\text{H}_{\text{pre}}$ was acquired at 9 long term stations located along the different aridity zones of Chile (IAEA/WMO, 2023). **A.** Residuals for the regression considering all month $\delta^2\text{H}_{\text{pre}}$ values registered for each station. **B.** Residuals for the regression considering the long-term $\delta^2\text{H}_{\text{pre}}$ average values for each month at every station. **C.** Considering the long-term $\delta^2\text{H}_{\text{pre}}$ average values for each month at every station. **D.** Residuals for the regression considering the long-term $\delta^2\text{H}_{\text{pre}}$ average values for each year at every station.

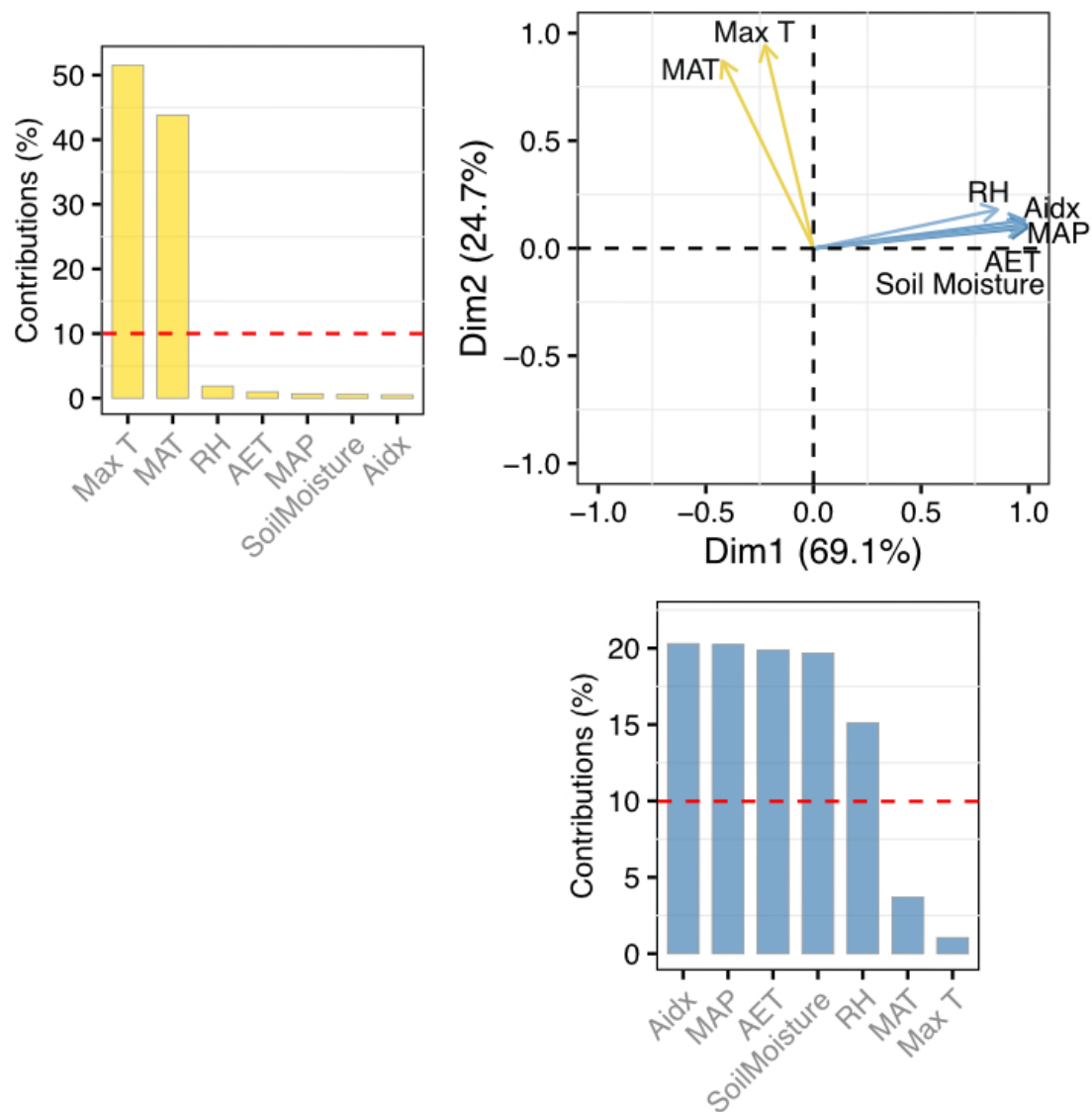


Figure S3. PCA plots and bar plots of PCA contributions for all the climatic variables considered in the study.

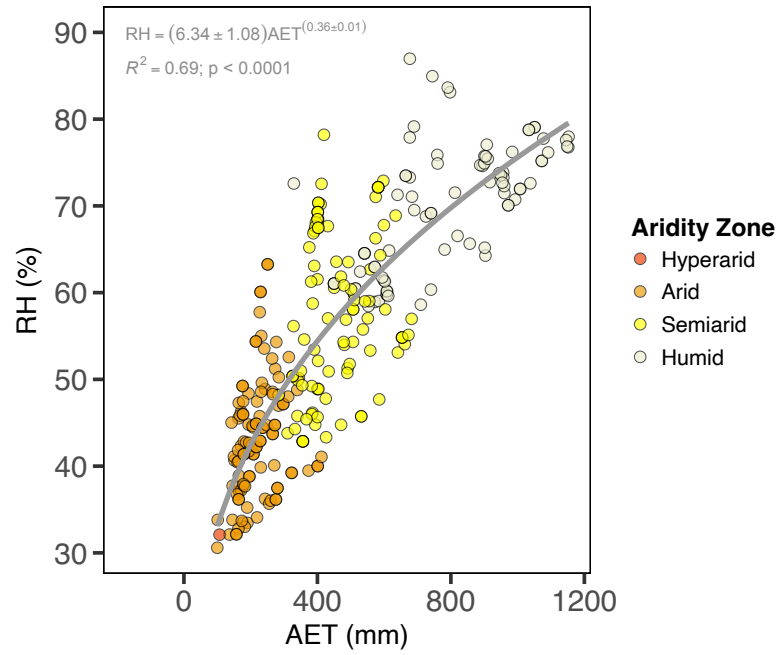


Figure S4. RH vs AET for the four aridity gradients selected from the global compilation (Table S2 in the data supplement). The power model fitted is used to parametrize RH as a function of AET in the model implemented in fig. 6 of the main text of the manuscript that this data publication accompanies.

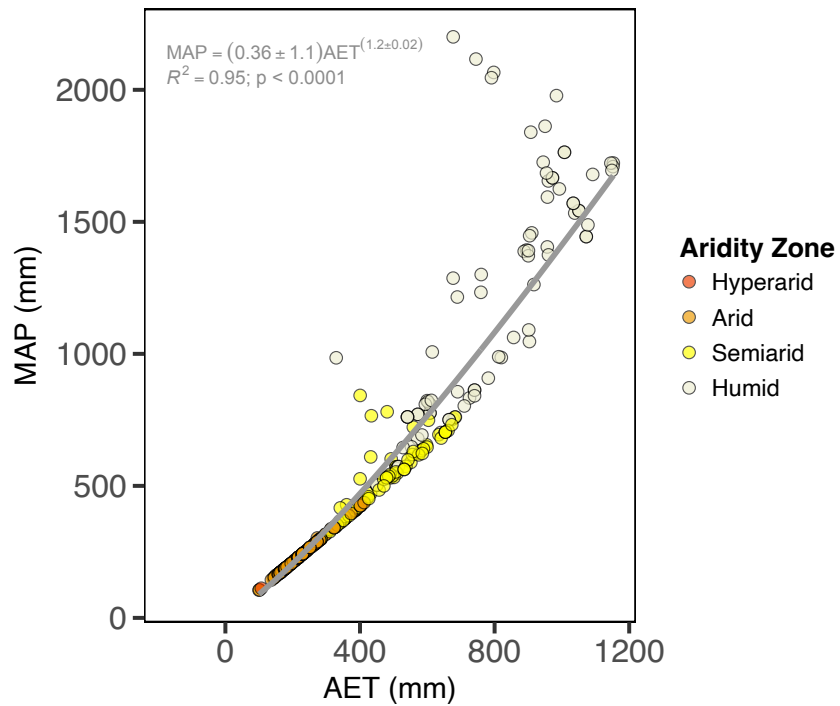


Figure S5. MAP vs AET for the four aridity gradients selected from the global compilation (Table S2 in the data supplement). The power model fitted is used to parametrize MAP as a function of AET in the model implemented in fig. 6 of the main text of the manuscript that this data publication accompanies.

References

Bowen, G. J. and Revenaugh, J.: Interpolating the isotopic composition of modern meteoric precipitation, *Water Resources Research*, 39, <https://doi.org/10.1029/2003WR002086>, 2003.

IAEA, W. (2023). IAEA/WMO, Global Network of Isotopes in Precipitation. The GNIP Database. <https://nucleus.iaea.org/wiser>